T. Magn. Soc. Jpn. (Special Issues)., **1**, 66-69 (2017)

<Paper>

Demagnetizing Analysis of Ferrite Magnet Motor Based on RNA

Y. Yoshida, D. Momma*, and K. Tajima
Graduate School of Engineering Science, Akita Univ., *1-1, Tegata Gakuen-machi, Akita 010–5802, Japan*
* Graduate School of Engineering and Resource Science, Akita Univ., *1-1, Tegata Gakuen-machi, Akita 010–5802, Japan*

A method for analyzing the demagnetization of a surface permanent magnet (SPM) motor based on reluctance network analysis (RNA) is presented. The validity of the proposed RNA model is demonstrated by comparing the calculated results with 2D-FEA calculation results. The characteristics of the SPM motor determined by the RNA model were in almost complete agreement with the corresponding two-dimensional (2D) finite element analysis (FEA) calculation.

Keywords: reluctance network analysis, ferrite magnet, demagnetization analysis, two-line approximation

1. Introduction

In recent years, high-performance permanent magnet (PM) motors based on powerful rare-earth magnets have emerged, and demand is consequently expanding in various applications. However, rare-earth magnets may be subject to price rises as the production of such metals tends to be concentrated in a single country. Therefore, the development of high-performance PM motors without rare-earth magnets is required.

Although the maximum magnetic energy product of ferrite magnets is one tenth that of rare-earth magnets [1], high-efficiency ferrite magnet motors have been reported [2]. Ferrite magnets in motors are exposed to a large reverse magnetic field to obtain performance equivalent to that of rare-earth magnet motors. Therefore, ferrite magnets are at risk of demagnetization because of their low coercive force. This makes it necessary to consider the demagnetization of ferrite magnets for ferrite magnet motor design.

Reluctance network analysis (RNA) is a useful method to save calculation time in the estimation of the characteristics of PM motors, as reported in previous studies [3)-6)]. In a previous paper, we proposed a demagnetization analysis method using RNA [7]. In that study, we presented an RNA model for determining the operating points of ferrite magnets taking account of a magnet's demagnetization. We demonstrated the calculation accuracy of this model, which used a two-line approximation of the demagnetization curve, by experiments and a comparison with two-dimensional (2D) finite element analysis (FEA). Therefore, in the present work, we apply this method to the demagnetization analysis of a surface permanent magnet (SPM) motor. To verify the accuracy of the proposed model, the calculated results are compared to values obtained from 2D FEA.

2. RNA model of SPM motor

Figure 1 shows the shape and specifications of the SPM motor under consideration. Stator and rotor core material is non-oriented electromagnetic steel sheet and the relative permeability of 3000 is used to calculate the reluctance in the RNA model. The material of the permanent magnet is ferrite (SSR-420).

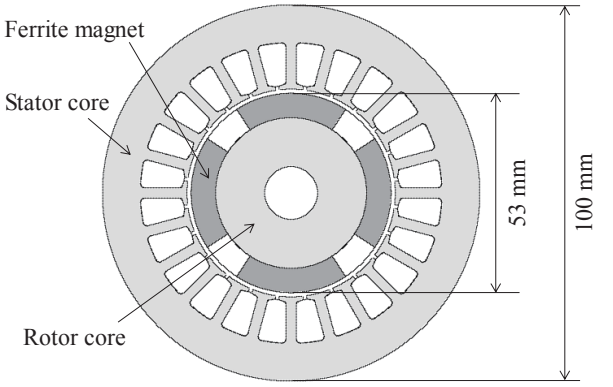

Number of slots	24
Number of poles	4
Core materials	Non-oriented electromagnetic steel sheet (Relative permeability $\mu_s = 3000$)
Permanent magnet materials	Ferrite magnet (SSR-420)
Number of winding turns per slot	100
Stack length	30 mm
Gap length	1.1 mm

Fig. 1 Shape and specifications of the SPM motor.

Figure 2 shows a part of the RNA model of the SPM motor. The SPM motor is divided into multiple elements taking into consideration the motor shapes and flux flow. Each element in the air gap is divided in one-degree intervals in the circumferential direction and the magnets are divided into three in the radial direction. The stator tooth tip is divided into three regions and reluctances in these regions are directly connected with air gap reluctances, as shown in the figure.

Figure 3 illustrates the demagnetization curve of SSR-420 at 20 °C used for the RNA model, which is approximated by two lines. In the figure, B_r, B_r', H_c, and H_c' are the residual magnetic flux density before demagnetization, residual magnetic flux density after demagnetization, coercive force before demagnetization, and coercive force after demagnetization, respectively. Since the demagnetization curve of the magnet is approximated by two lines, there is a slight error around the knee point.

The elements of a ferrite magnet of the RNA model

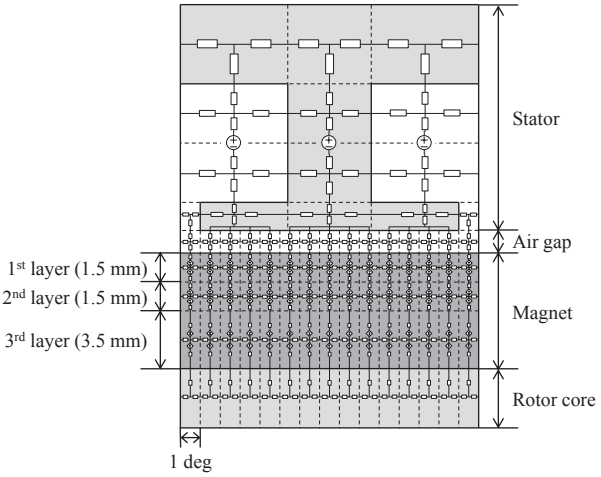

Fig. 2 A part of the RNA model.

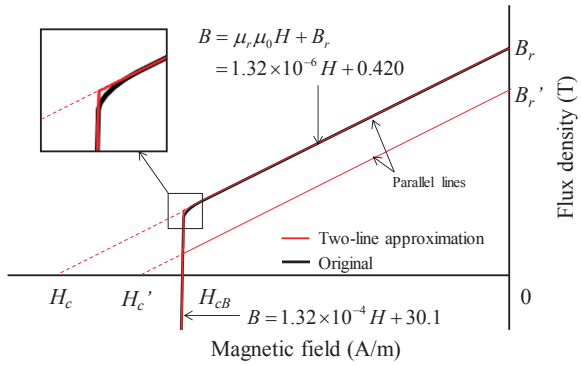

Fig. 3 Demagnetization curve of SSR-420 at 20 °C.

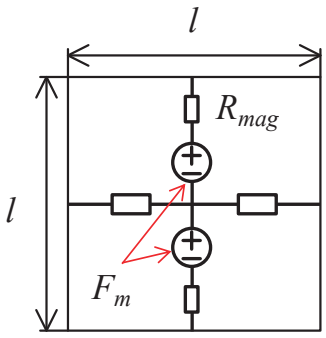

Fig. 4 Unit magnetic circuit of magnet element.

can be expressed as the reluctance and magnetomotive forces (MMFs), F_m, shown in Fig. 4. The reluctance of a ferrite magnet, R_{mag}, is expressed by

$$R_{mag} = \frac{l}{2\mu_r\mu_0(l \times l_s)}, \quad (1)$$

where μ_r is the magnet's recoil. If there is no demagnetization in a ferrite magnet element, F_m is given by

$$F_m = \frac{B_r l}{2\mu_r\mu_0}. \quad (2)$$

When an operating point of a ferrite magnet is changed by an external magnetic field and becomes less than the knee point, the MMF after demagnetization, F_m', can be expressed as

$$F_m' = \frac{B_r' l}{2\mu_r\mu_0}. \quad (3)$$

3. Demagnetization analysis of SPM motor

Using the derived RNA model, the characteristics of the SPM motor are calculated taking demagnetization into account. To verify the calculation accuracy of the RNA model, the calculated values were compared to the ones obtained from 2D-FEA (JMAG-Designer Ver.15).

Figure 5 shows the 2D-FEA model of the SPM as a comparison object. Figure 6 shows the comparison of the calculated waveforms of flux linkage. It is clear that the calculated values obtained from the proposed RNA model are in good agreement with the ones obtained from 2D-FEA.

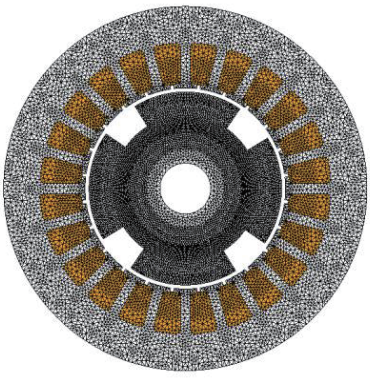

Fig. 5 2D FEA model of the SPM motor.

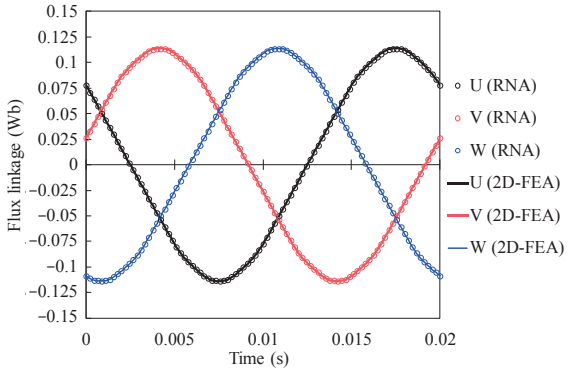

Fig. 6 Comparison of the flux linkage calculated by proposed model and 2D-FEA.

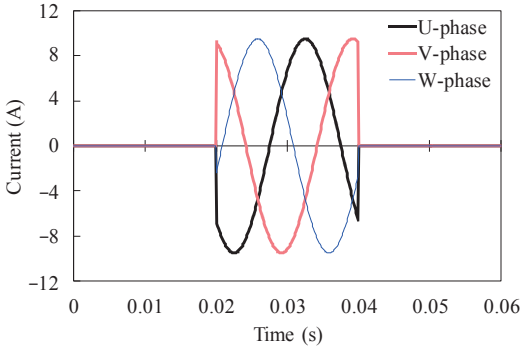

Fig. 7 Input current wave forms for calculating induced voltage of the SPM motor.

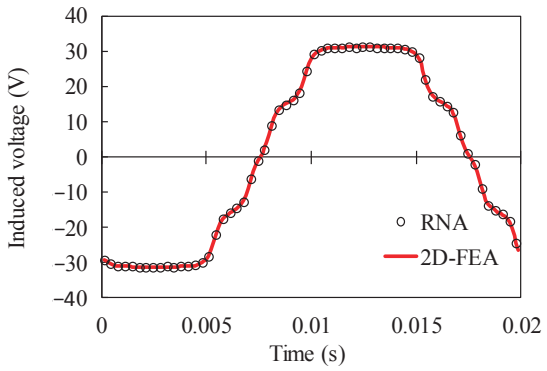

(a) Before demagnetization

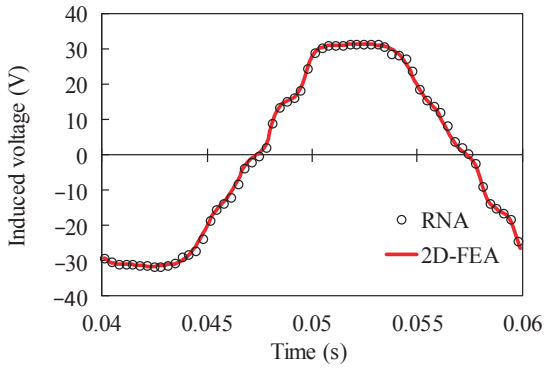

(b) After demagnetization

Fig. 8 Comparison of U-phase induced voltage between RNA and FEA.

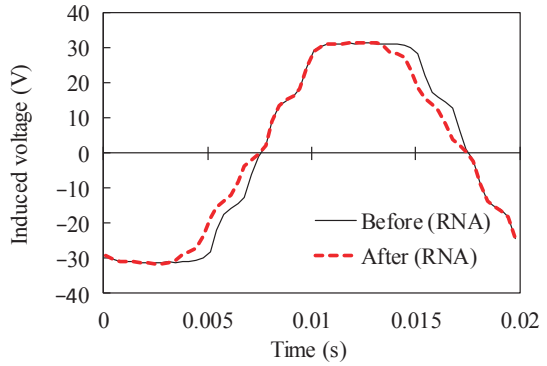

Fig. 9 Comparison of U-phase induced voltage before and after demagnetization.

Next, the induced voltages of the SPM motor before and after demagnetization are calculated. Figure 7 shows the three periods of input current wave forms. In the first and third periods, the rotor rotates at the rotor speed of 1500 rpm without supplying current. In the second period (0.02 seconds to 0.04 seconds), the overcurrent at the amplitude of 9.5 A is applied; rated current amplitude of this SPM motor is 4.0 A.

Figure 8(a) and (b) shows the comparison of calculated induced voltage before and after demagnetization between RNA and FEA, respectively. In these figures, the calculated values obtained from the proposed RNA model are in good agreement with the ones obtained from 2D FEA. Figure 9 shows the comparison of calculated induced voltage by RNA before and after demagnetization. The amplitude of the fundamental wave of the induce voltage after demagnetization is decreased by 5.7 % and the phase of the fundamental wave is shifted by 5.5 degrees compared to the induced voltage before demagnetization.

To compare the torque of the SPM motor before and after demagnetization, three periods of input current

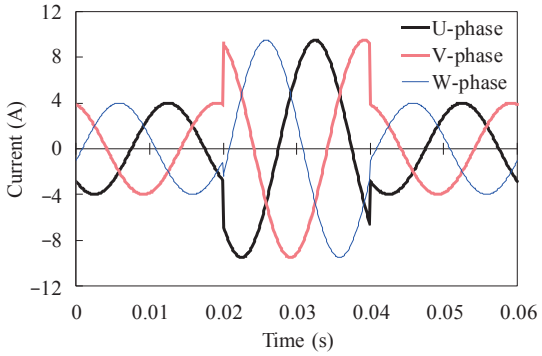

Fig. 10 Input current wave forms for calculating torque of the SPM motor.

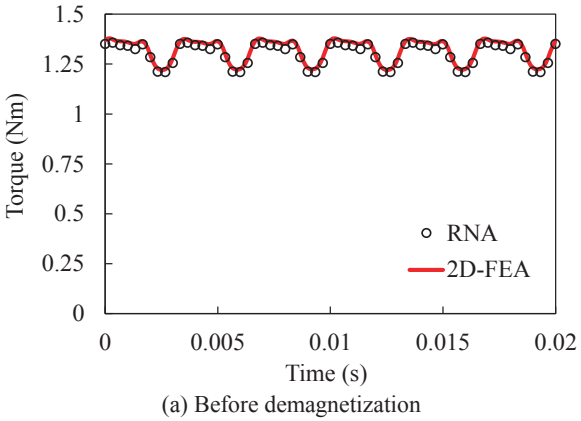

(a) Before demagnetization

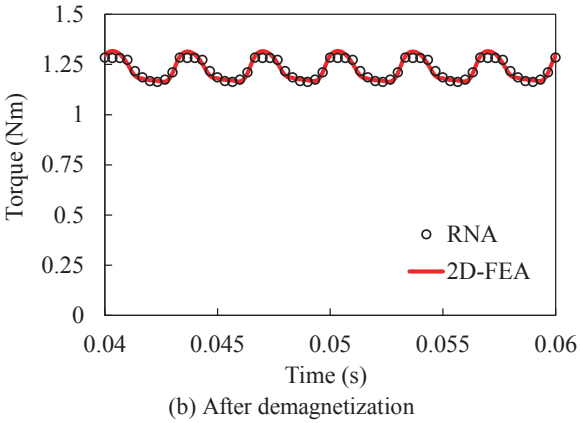

(b) After demagnetization

Fig. 11 Comparison of torque waveform of the SPM motor.

Table 1 Comparison of average torque.

	RNA (Nm)	2D-FEA (Nm)	Error (%)
Before	1.30	1.32	1.51
After	1.22	1.23	0.813

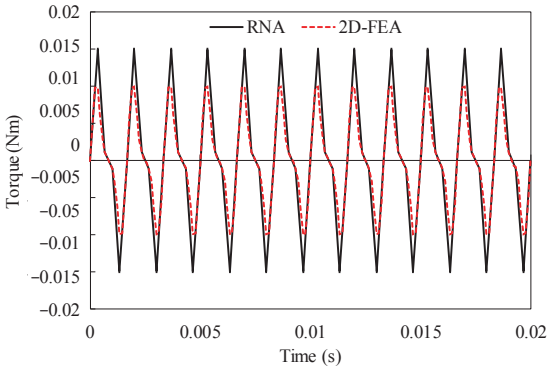

(a) Before demagnetization

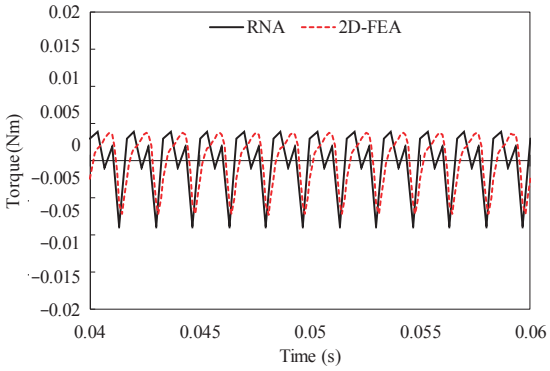

(b) After demagnetization

Fig. 12 Comparison of cogging torque before and after demagnetization.

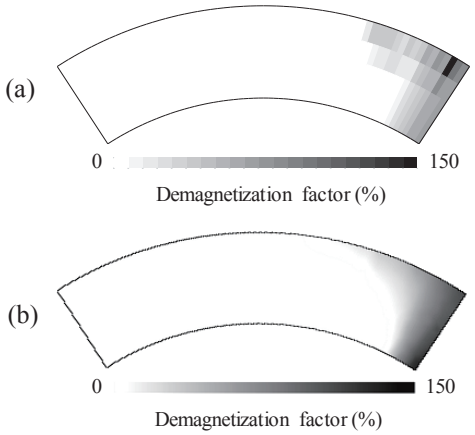

Fig. 13 Demagnetization factor of the ferrite magnet calculated by RNA (a) and 2D-FEA (b).

wave forms are used, as shown in Fig. 10. In the first period, the current amplitude of 4.0 A is applied to the motor to calculate the rated torque before demagnetization. To demagnetize the rotor magnets, the overcurrent more than double the rated current (9.5 A) is supplied in the second period. Then, the current at the amplitude of 4.0 A is applied again to calculate the rated torque after demagnetization in the last period.

Figure 11 shows the comparison of the torque wave forms of the SPM motor calculated by the proposed RNA model and 2D-FEA. In the figures, the calculated values obtained from the proposed RNA model are in almost complete agreement with the ones obtained from 2D-FEA.

Table 1 lists the average torque before and after demagnetization. The average torque calculated by the RNA model is decreased by 6.2 % compared to before demagnetization. The errors of the average torque between the RNA model and 2D FEA are less than 2 %.

Figure 12(a) shows the cogging torque waveform before demagnetization and Fig. 12(b) shows the cogging torque waveform after demagnetization calculated using the input current waveforms shown in Fig. 7. After demagnetization, there is a bit of a discrepancy in the cogging torque waveforms between RNA and 2D-FEA. Figure 13 shows the demagnetization factor calculated by RNA and 2D-FEA, where the demagnetization factor, D_{fac}, is defined as

$$D_{fac} = \left(1 - \frac{B_r'}{B_r}\right) \times 100 \cdot \qquad (4)$$

Comparing these results, the demagnetization factor of the surface of the magnet calculated by the RNA is larger than the one obtained from 2D-FEA. We conclude that the discrepancy in the distribution of the demagnetization factor affects the cogging torque waveforms.

4. Conclusion

This study presented a method for demagnetization of the SPM motor based on RNA. The validity of the proposed RNA model was demonstrated by comparing the calculated results with 2D-FEA calculation results. It is concluded that the characteristics of the SPM motor determined by the RNA model are in almost complete agreement with the corresponding 2D-FEM calculated. Further studies will attempt to perform demagnetization analysis considering the effect of the distorted current waveform by voltage input.

This work was supported by JSPS KAKENHI Grant Number 26820093.

References

1) M. Sagawa, M. Hamano, and M. Hirabayashi: Eikyujishaku –Zairyokagaku to Oyo– (in Japanese), p. 16 (Agune Gijutsu Center, Tokyo, 2007).
2) M. Sanada, Y. Inoue, and S. Morimoto: *IEEJ Trans. IA*, **131**, 12, 1401–1407 (2011).
3) K. Nakamura, K. Saito, and O. Ichinokura: *IEEE Trans. Magn.*, **39**, 3250–3252 (2003).
4) K. Nakamura, M. Ishihara, and O. Ichinokura: *17th International Conference on Electrical Machines (ICEM 2006)*, PSA1-16 (2006).
5) K. Nakamura and O. Ichinokura: *13th International Power Electronics and Motion Control Conference (EPE-PEMC 2008)*, 441 (2008).
6) Y. Yoshida, K. Nakamura, O. Ichinokura, and K. Tajima: *IEEJ Journal IA*, 3, 6, 422–427 (2014).
7) D. Momma, Y. Yoshida, and K. Tajima: J. Magn. Soc. Jpn., **40**, 115–119 (2016).

Received October 20, 2016; Revised November 24, 2016; Accepted January 4, 2017.